4/

A Life-Cycle of Nonlinear Baroclinic Waves Represented by 3-D Spectral Model

H. L. Tanaka
University of Tsukuba, Tsukuba 305 Japan

1. INTRODUCTION

Simmons and Hoskins (1978) conducted a numerical simulation of a life-cycle of nonlinear baroclinic waves. According to their simulations, an initial perturbation superimposed on a zonal field grows exponentially by baroclinic instability drawing zonal available potential energy. The amplified baroclinic waves start to transfer the energy back to the zonal kinetic energy by the barotropic conversion. The nonlinear baroclinic waves appear to accelerate the zonal jet at the end of their life-cycle as an expense of the zonal available potential energy.

There should be no contradiction between the relaxed meridional temperature gradient and the accelerated zonal jet with reference to the thermal wind relation. The acceleration of zonal wind is supposed to occur at the lower troposphere and deceleration at the tropopause level so that the wind shear diminishes. In this regard, more detailed analysis would be necessary to understand the role of the baroclinic disturbances for the changes in the vertical structures of zonal and eddy fields.

In the present study, the life-cycle experiment is demonstrated for Simmons and Hoskins' 45°jet with initial perturbations of zonal wavenumber n=6 by integrating the three-dimensional spectral primitive equation model (see Tanaka, 1991). Here, the vertical normal mode expansion is applied for the discretization of governing equations in the vertical, which is straightforward for the analysis of energy redistribution in the vertical spectral domain. We analyze the energy transfer within the vertical spectral domain associated with the life-cycle of the baroclinic disturbances. The energy evolution and corresponding energy transformations are presented in the framework of baroclinic-barotropic decomposition of atmospheric energy.

2. MODEL DESCRIPTION

A system of primitive equations in a spherical coordinate of longitude λ, latitude θ, normalized pressure $\sigma = p/p_b$, and normalized time $\tau = 2\Omega t$ may be reduced to three prognostic equations of horizontal motions and thermodynamics. The three dependent variables are horizontal wind speeds, $V = (u, v)$, and geopotential deviation ϕ from the global mean reference state. Here, p_b and Ω are bottom pressure of the reference state and angular speed of Earth's rotation, respectively. Using a matrix notation, these equations (refer to Tanaka and Sun 1990) may be written as:

$$M\frac{\partial}{\partial\tau}U + LU = N + F, \tag{1}$$

where

$$U = (u, v, \phi)^T, \tag{2}$$

The symbols M and L designate linear matrix differential operators with respect to the vertical and horizontal domains, N the nonlinear advection terms, and F the diabatic processes including frictional forces.

A 3-D spectral representation of the primitive equations can be derived by taking an inner product of (1) and basis functions of the 3-D normal mode functions $\Pi_{nlm}(\lambda, \theta, \sigma)$:

$$< M\frac{\partial}{\partial\tau}U + LU - N - F,\ Y_m^{-1}\Pi_{nlm} >= 0, \tag{3}$$

where

$$\Pi_{nlm}(\lambda, \theta, \sigma) = H_{nlm}(\lambda, \theta)\, G_m(\sigma), \tag{4}$$

$$Y_m = 2\Omega\, diag(\sqrt{g\,h_m},\ \sqrt{g\,h_m},\ 1), \tag{5}$$

and the inner product is defined as

$$\frac{1}{2\pi}\int_{-\pi/2}^{\pi/2}\int_0^{2\pi}\int_0^1 \Pi^*_{nlm}\cdot\Pi_{n'l'm'}\, cos\theta d\sigma d\lambda d\theta$$
$$=< \Pi_{nlm},\ \Pi_{n'l'm'} >= \delta_{nn'}\,\delta_{ll'}\,\delta_{mm'}. \tag{6}$$

Here, $H_{nlm}(\lambda, \theta)$ and $G_m(\sigma)$ are Hough harmonics and vertical structure functions for zonal wavenumber n, meridional index l, and vertical index m, respectively. These three indices will be reduced to a single index i for short. The scaling matrix Y_m is defined with the Earth's gravity g, and equivalent height h_m, for every vertical index. Refer to Tanaka and Sun (1990) for the detail of the definitions and the derivation.

The resulting spectral primitive equations become a system of ordinary differential equations for Fourier expansion coefficients of variables:

$$\frac{dw_i}{d\tau} + i\sigma_i w_i = -i\sum_{j=1}^{M}\sum_{k=1}^{M} r_{ijk}w_j w_k + f_i,$$
$$i = 1, 2, ..., M, \tag{7}$$

where w_i and f_i are the expansion coefficients of the dependent variables and diabatic processes, σ_i are Laplace's tidal frequencies, r_{ijk} are interaction coefficients, and M is the total number of the series expansion for the 3-D atmospheric variables.

In this study, we consider diffusion DF as a single physical process. The scale dependency of diffusion is parameterized using the 3-D scale index σ_i based on the wave dispersion relating the wave scale and wave frequency. We approximate biharmonic-type diffusion for the Rossby (rotational) wave dispersion (for wavenumber $n \neq 0$) by:

$$(DF)_i = -K(\frac{n}{\sigma_i})^2 w_i, \tag{8}$$

where K is a diffusion coefficient. Haurwitz waves on a sphere have phase speeds represented by the total wavenumber of the spherical surface harmonics $\hat{l}$ (see Swarztrauber and Kasahara 1985):

$$c = \frac{-1}{\hat{l}(\hat{l}+1)} \simeq \frac{\sigma_i}{n}. \tag{9}$$

Since the diffusion is often approximated with $\hat{l}(\hat{l}+1)$, the present form of diffusion in (8) tends to be the biharmonic-type diffusion for higher order Rossby modes. For the zonal component, the meridional index l_R is substituted for $\hat{l}$.

The system of nonlinear equations (7) is truncated to include only the Rossby modes for m=0-6, n=0 and 6, and l_R=0-19. Note that the truncation is imposed in the frequency domain as well as in the wavenumber domain by excluding high-frequency gravity modes.

The initial condition is a northern zonal field of January 1979 which is assumed to be symmetric about the equator. Small amplitude unstable normal modes are superimposed on the initial zonal field. The time integration is based on a combination of leap-frog and a periodic use of Euler-backward scheme. By virtue of the closure with the low-frequency subspace, our model requires no implicit scheme and no artificial smoothing.

3. ENERGETICS ANALYSIS

The total energy, E_i for each basis function is defined in a dimensional form by

$$E_i = \frac{1}{2} p_b h_m |w_i|^2. \tag{10}$$

In order to explore the origin of this energy supply, an energy flow box diagram describing energy interactions between barotropic and baroclinic components is constructed. By differentiating (10) with respect to time and substituting (7), we obtain for eddy:

$$\begin{aligned} \frac{dE_i}{dt} &= 2\Omega p_b h_m \textstyle\sum_j Re(ib_{ij}^* w_j^* w_i)_{m''=0} \\ &+ 2\Omega p_b h_m \textstyle\sum_j Re(ib_{ij}^* w_j^* w_i)_{m''\neq 0} \\ &= C(B_{m''=0}, E_i) + C(B_{m''\neq 0}, E_i). \end{aligned} \tag{11}$$

Note that the linear term in the left-hand side of (7) does not contribute to the energy balance equation. The first term of the right-hand side of (11) stands for energy transformations from the barotropic component of the zonal field $B_{m''=0}$ into E_i, and the second term represents those from the baroclinic components of the zonal field $B_{m''\neq 0}$ into E_i. By adding all indices for m=0, and for $m \neq 0$, (11) becomes:

$$\frac{dE_{m=0}}{dt} = C(B_{m''=0}, E_{m=0}) + C(B_{m''\neq 0}, E_{m=0}), \tag{12}$$

$$\frac{dE_{m\neq 0}}{dt} = C(B_{m''=0}, E_{m\neq 0}) + C(B_{m''\neq 0}, E_{m\neq 0}). \tag{13}$$

The resulting energy flow box-diagrams are presented in Fig. 1 for the most unstable Charney mode at n=6. Upper boxes ($m'' \neq 0, m \neq 0$) denote the baroclinic component and lower boxes ($m'' = 0, m = 0$) the barotropic components. It is shown that large proportions of energy are transformed from zonal baroclinic energy to eddy baroclinic energy then to eddy barotropic energy for the growing modes. The result with FGGE observation represents the characteristics of energy flow by the baroclinically unstable modes.

4. RESULTS OF THE SIMULATION

Figure 2 shows the time variations of energy and energy conversions discussed in Fig.1 for the life-cycle of the nonlinear baroclinic disturbances. As shown in Fig. 2, the initial perturbations of n=6 grow exponentially drawing zonal baroclinic energy. This early evolution is reasonably described by linear baroclinic instability of the 45°jet. Both the baroclinic energy and barotropic energy of n=6 increase simultaneously since the unstable mode maintains its consistent structure to grow. The energy flow is characterized as from zonal baroclinic energy via eddy baroclinic energy and to eddy barotropic energy. These energy transformations are also synchronized since they are proportional to the eddy energy levels in the linear framework.

When the waves reach finite amplitude, barotropic conversion increases, transferring the accumulated eddy barotropic energy toward zonal barotropic energy. As the result, zonal barotropic energy increases when the synoptic waves decay. It is shown that the zonal jet is accelerated so that the structure becomes more barotropic. The results are consistent with previous studies.

The important process in baroclinic instability is the eddy heat flux due to the zonal-wave interaction and simultaneous baroclinic conversion at each zonal

Fig.1 Energy flow box diagram within zonal and eddy energies decomposed in barotropic and baroclinic components. (a) FGGE observation, (b) unstable Charney mode for n=6. Units are $10^5 \mathrm{Jm}^{-2}$ for energy and Wm^{-2} for energy conversions. Percentile contributions are substituted for (b).

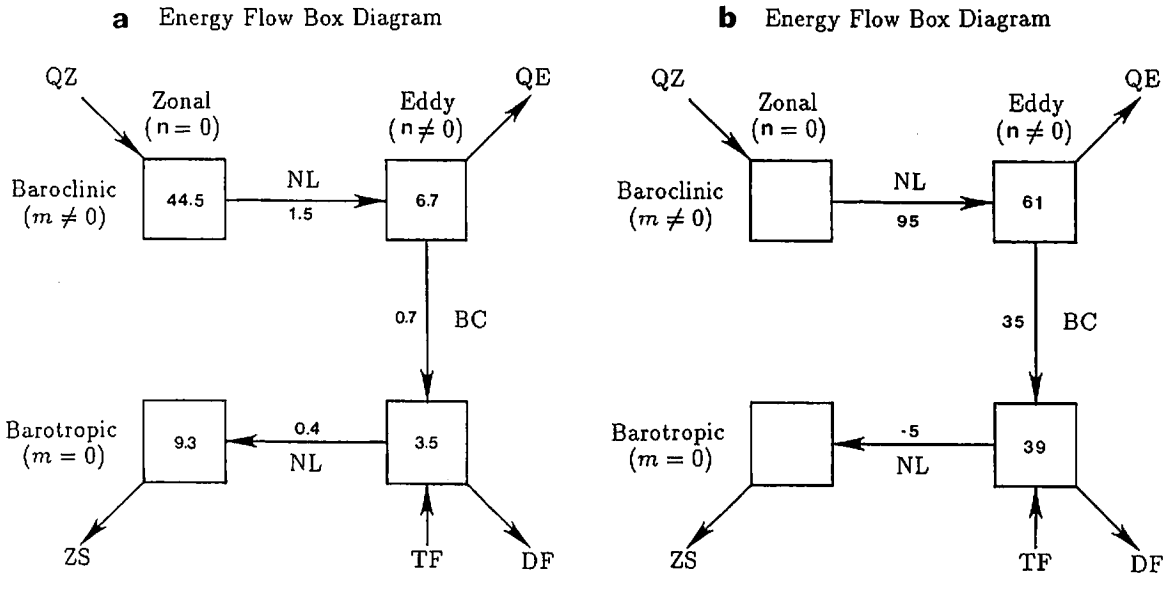

wavenumber. This baroclinic conversion is fundamentally a linear process. In contrast, the up-scale zonal-wave interaction of the barotropic conversion is essentially a nonlinear process. We find that the important baroclinic-barotropic interactions are coupled with baroclinic instability rather than the barotropic conversion.

Figure 3 illustrates the time variations of energy and energy conversions as seen in Fig. 2. During this simulation, the largest meridional components of the zonal baroclinic field (m=4) are fixed as steady to maintain the meridional temperature gradient. The diffusion coefficient is increased in order to balance with the increased energy supply. As the result, we find that the baroclinic disturbances repeat the life-cycle for several times, drawing the energy from the zonal baroclinic components and feeding the zonal barotropic jet. The role of the baroclinic disturbances is therefore evident to pump the zonal energy from the baroclinic to the barotropic components.

5. CONCLUDING REMARKS

A life-cycle of nonlinear baroclinic waves is examined in terms of the barotropic-baroclinic decomposition of zonal and eddy fields. We can clearly observe the time lag between the relaxation of the meridional temperature gradient and the acceleration of the zonal jet due to the activities of the nonlinear baroclinic disturbances. The jet is accelerated so that the structure becomes more barotropic in the vertical. This means that the zonal wind is accelerated at the lower troposphere, where the frictional dissipation is most efficient.

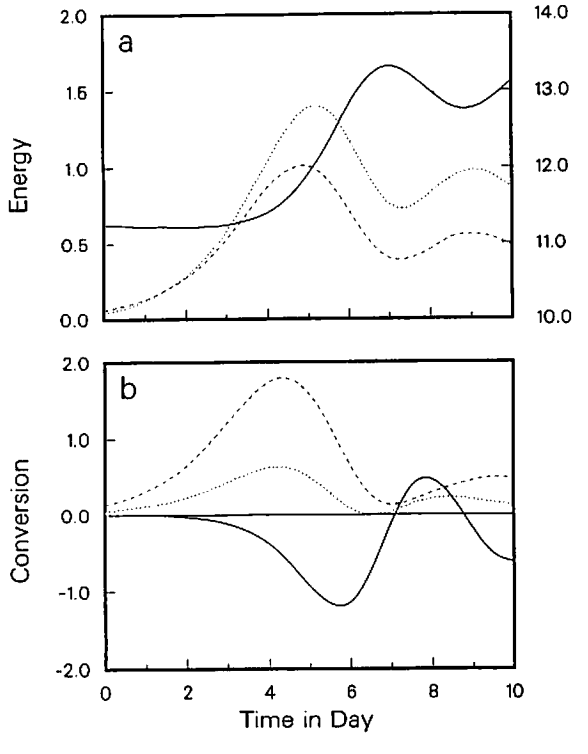

Fig.2 (a) Time variations of eddy baroclinic energy (dashed line), eddy barotropic energy (dotted line), and zonal barotropic energy (solid line with its scale at right ordinate) for n=6. Units are $10^5 \mathrm{Jm}^{-2}$. (b) Time variation of energy conversion from zonal baroclinic to eddy baroclinic energies (dashed line), from eddy baroclinic to eddy barotropic energies (dotted line), and from eddy barotropic to zonal barotropic energies (solid line). Units are Wm^{-2}.

It is concluded by this study that the role of the nonlinear baroclinic disturbances is to convert the zonal baroclinic energy toward the barotropic component of motions so that the energy is most efficiently dissipated by the frictional drag near the ground.

Acknowledgments

This research is jointly supported by the Sumitomo Foundation under the contract number 93-104-457 and by Grant-In-Aid from the Ministry of Education under the number 05NP0203. The author is grateful to K. Itoh for the technical assistance.

References

Swarztrauber, P.N., and A. Kasahara, 1985: The vector harmonic analysis of Laplace's tidal equation. *SIAM J. Sci. Stat. Comput.*, **6**, 464-491.

Simmons, A. J., and B. Hoskins, 1978: The life cycles of some nonlinear baroclinic waves. *J. Atmos. Sci.*, **35**, 414-432.

Tanaka, H. L., and S. Sun, 1990: A study of baroclinic energy sources for large-scale atmospheric normal modes. *J. Atmos. Sci.*, **47**, 2674-2695.

Tanaka, H.L., 1991: A numerical simulation of amplification of low-frequency planetary waves and blocking formations by the upscale energy cascade. *Mon. Wea. Rev.*, **119**, 2919-2935.

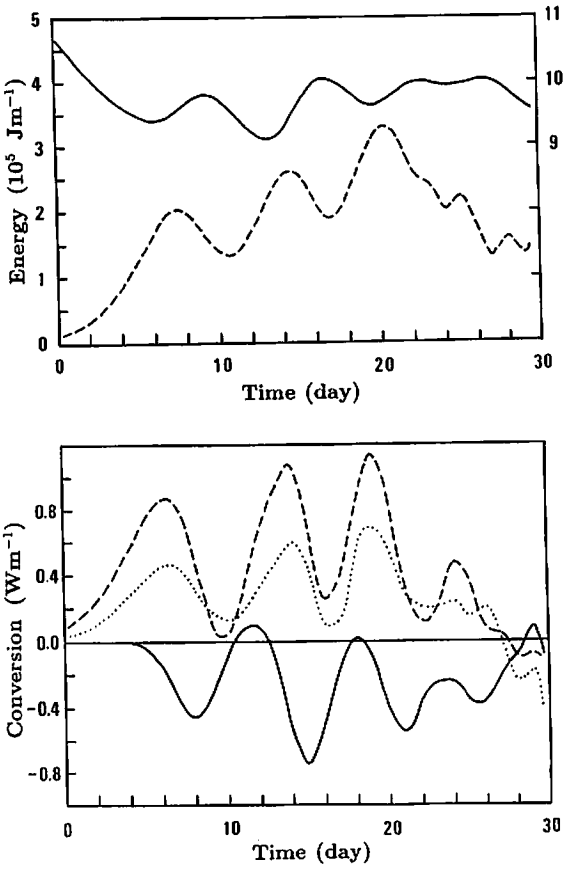

Fig.3 Time variations of energy and energy conversion as in Fig.2, but for an experiment with restoring zonal baroclinic field. The eddy energy (dashed line) is the sum of the barotropic and baroclinic components.